Journal of Applied Polymer Science

Preparation of Oligo-*N*-isopropylacrylamide Brushes with —OH and —COOH End-Groups via Surface-Initiated NMP

Dilek Cimen, Tuncer Caykara
Department of Chemistry, Faculty of Science, Gazi University, 06500 Besevler, Ankara, Turkey
Correspondence to: T. Caykara (E-mail: caykara@gazi.edu.tr)

ABSTRACT: Functional brushes have recently emerged as an extremely versatile way to modify surface properties in a robust and controlled way. In this study, well-defined, high density oligo-*N*-isopropylacrylamide (oligoNIPAM) brushes with —OH and —COOH end-groups were fabricated through a reliable strategy by the combination of the self-assembly of bimolecular macroazoinitiator on silicon surface and surface-initiated nitroxide mediated polymerization of *N*-isopropylacrylamide in the presence of chain transfer agent (i.e., 2-mercaptoethanol or 3-mercaptopropionic acid). The living polymerization produced silicon substrate-coated with functional oligoNIPAM with a target molecular weight and a grafting density as high as 8.14 chains nm^{-2}. The functional oligoNIPAM brushes can be employed for the adsorption of biomacromolecules such as DNA and proteins. © 2012 Wiley Periodicals, Inc. J. Appl. Polym. Sci. 129: 383–390, 2013

KEYWORDS: applications; monolayers and polymer brushes; properties and characterization; radical polymerization; spectroscopy

Received 17 August 2012; accepted 19 October 2012; published online 16 November 2012
DOI: 10.1002/app.38741

INTRODUCTION

The functionalization of silicon wafer or gold nanoparticles by grafting of polymer chains to the surface provides a powerful and flexible route to improve the physical and chemical properties of substrates.[1–3] The importance of the functional surfaces is highlighted by the use of an increasing number of applications ranging from biosensors[4] and the use of biomolecules which control the self-assembly of nanodevices,[5] to the fabrication of implants showing bioactivity for the regeneration of damaged tissues.[6–8]

These applications commonly require the interaction between biomolecules, cells or tissues and solid substrates by means of a stable intermediate layer. The interlayer should provide adequate functional groups that react with biomolecules. The most functional groups are —OH, —COOH, and —SH that interact readily with biomolecules by covalent bonding. Because of its relevance, the development of protein immobilization, nucleic acid detection (RNA and DNA), biocatalysis, tissue engineering, etc., will rely on advances in the preparation of functional surfaces.

Using a "grafting from" method with living/controlled radical polymerization enables preparation of solid substrates with functional end-groups and high grafting density, controlled graft structure/composition and applicability to different monomers.[9,11] The studies in this area have focused on surface modification of silicon wafer or gold nanoparticles by atom transfer radical polymerization (ATRP)[12–19] or reversible addition-fragmentation transfer (RAFT) polymerization.[20–22] However, surface-initiated NMP has the advantage of being a relatively simple process, although it is not as versatile as ATRP or RAFT in the range of monomers suitable for use. Although many studies were reported on the surface-initiated NMP, only polystyrene or poly(2-(dimethylamino)ethyl acrylate) was grafted onto the silicon wafer or gold nanoparticle surfaces.[23–29] Grafting of polymer chains with defined end-groups on silicon wafer or gold nanoparticle surfaces by surface-initiated NMP can bring about enhanced properties such as hydrophilicity, hydrophobicity, and even a smart response to environmental changes (pH, temperature, solvent composition, etc.), enabling the preparation of substrates with more widespread application.

Poly(*N*-isopropylacrylamide) [poly(NIPAM)], a temperature-responsive polymer, is well known to exhibit reversible hydration and dehydration of its polymer chains in response to temperature changes across the lower critical solution temperature (LCST) of 32°C.[30,31] However, the kinetics are not very sensitive to temperature for the lower molecular weight (1.3×10^4 g mol^{-1}) poly(NIPAM), in contrast to the higher molecular weight (5×10^5 g mol^{-1}) polymer.[32] Yim et al. reported no temperature-dependent conformational change with the lowest molecular weight poly(NIPAM) (3.3×10^4 g mol^{-1}), and only a slight temperature dependent thickness change with the higher molecular weight polymer (2.2×10^5 g mol^{-1}).[33] Despite the

poly(NIPAM) with lower molecular weight has no temperature-dependent conformational change, it exhibits good protein resistance at room temperature.[34,35] Moreover, a highly homogeneous surface with a roughness less than the height of the adsorbed protein molecules is also desired in most biosensing applications.[36] In this case, a thicker poly(NIPAM) or oligo-*N*-isopropylacrylamide (oligoNIPAM) brush would be more ideally suited for protein immobilization.

In this study, the synthesis of oligoNIPAM brushes with —OH and —COOH end-groups on silicon wafer was been conducted via surface-initiated NMP based on "grafting from" method, which provided a novel way to prepare densely packed and chemically attached oligo-brushes by *in* situ grafting oligomer chains from substrate surface. The surface-initiated NMP procedure allows control over the thickness of oligomers grown from a surface by varying reaction time. However, we chose to use the chain transfer agent, which both acts functional end-group forming agent during reaction and controls over film thickness and architectural parameters (e.g., grafting density, σ, chains nm^{-2}) of grafted chains. To the best of our knowledge, this is first example of the formation of well-defined oligoNIPAM brushes with functional end-group by surface-initiated NMP in the presence of chain transfer agent. We also elucidate how the type of chain transfer agent influence the molecular weight characteristics, film thickness, grafting parameters, surface morphology and wettability of the oligoNIPAM brushes with functional end-group. Finally, functional oligoNIPAM brushes can be employed to immobilize a range of antigens or ligands for biosensing applications and to work cell–surface interactions.

MATERIALS AND METHODS

Materials

NIPAM (Aldrich, Steinheim, Germany, 99.1%) was purified by recrystallization in a mixture of benzene/n-hexane. Ethanol (Aldrich, 96%), dichloromethane (Aldrich, 99%), 2-mercaptoethanol (ME, Aldrich, 99%), 3-mercaptopropionic acid (MPA, Aldrich, 99%), 3-aminopropyltrimetoxysilane (APTS, Aldrich, 97%) 4,4'-azobis-4-cyanopentanoic acid (ACPA) (Fluka, Steinheim, Germany, 97%) were used as received. Triethylamine (Aldrich, 99.5%) was distilled from calcium hydride under an argon atmosphere at reduced pressure. Tetrahydrofuran (THF, Aldrich, 99%) was purified by distillation from calcium hydride followed by distillation from sodium/benzophenone kethyl.

Synthesis of Bimolecular Macroazoinitiator

The 4,4'-azobis-4-cyanopentanoyl chloride (ACPC) was prepared according to the literature procedure described by Smith.[37]

^{1}H NMR (300 MHz, $CDCl_3$, δ, ppm): 1.67 (s, 3H, —CH_3—C(CN)—), 1.75 (s, 3H, —CH_3—C(CN)—), ~ 2.30–2.79 (m, 4H, —CH_2—CO—), ~ 2.86–3.20 (m, 4H, —CH_2—C(CN)CH_3—) [Figure 1(A)].

Then 3.0 g of ACPC was dissolved in 100 mL of anhydrous dichloromethane under nitrogen atmosphere and cooled to 0°C in an ice bath. Nearly 1.7 mL of APTS and 1.4 mL of triethylamine were added to the cold solution over 10 min, the solution was stirred in a dark place. After 3 h, the solution was allowed to come to room temperature and stirred with a mechanical stirring overnight. The solution was then centrifuged for 1 h at 5000 rpm and filtered through filter paper and the liquid part was stored at 4°C before use.

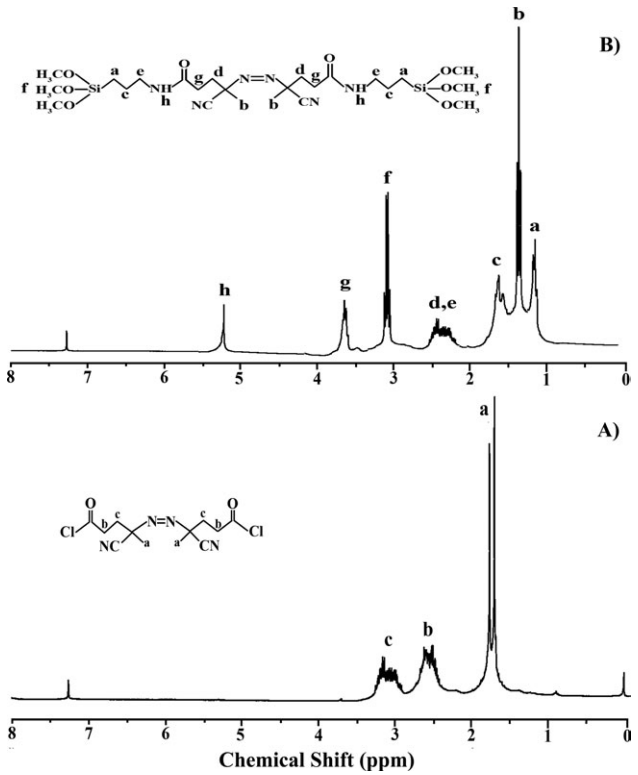

Figure 1. ^{1}H NMR spectra of ACPC (A) and bimolecular macroazoinitiator (B).

^{1}H NMR (300 MHz, $CDCl_3$, δ, ppm): 5.28 (s, 1H, —NH—CO—), 3.53 (m, 4H, —CH_2—CO—), 3.05 (t, 18H, —Si—OCH_3—), 2.56 (m, 4H, —CH_2—NH—), 2.32 (m, 4H, —CH_2—C(CN)CH_3—), 1.58 (m, 4H, —CH_2—CH_2—Si—), 1.33 (t, 6H, —CH_3—C(CN)—), 1.20 (t, 4H, —CH_2—Si—) [Figure 1(B)].

Immobilization of Bimolecular Macroazoinitiator

Silicon wafers (*n*-type, with a thickness of 0.5 mm, a diameter of 125 mm and polished on one side, Shin-etsu, Handoutai, Japan) were cut into 10 mm × 10 mm pieces, cleaned with acetone, and treated with a mixture of NH_4OH : H_2O_2 : H_2O (1 : 1 : 5 v/v) in an ultrasonic bath at 65°C for 30 min. They were then rinsed copiously with deionized water and blown dry with nitrogen. The polished sides of the wafers were also oxidized for 5 min in a UV/O_3 cleaner (Jelight Company; Irvine, CA: Model 42). Hydroxyls on the wafer surface were obtained by boiling the oxidized silicon wafers for 1 h in deionized water. The wafers treated this way are rich in hydroxyls at the oxide surface and suitable for the silanization process. The wafers were then dried well with nitrogen gas and placed into a solution of bimolecular macroazoinitiator (10 mL) in dry dichloromethane (10 mL). The flask was sealed with a rubber septum and waited in the refrigerator for 2.5 h. The wafers were removed from the solution and repeatedly washed with ethanol and dichloromethane, and dried under a stream of nitrogen. Bimolecular macroazoinitiator immobilization was apparent from the appearance of a carbonyl peak at 1630 cm^{-1} in the GA-FTIR spectrum of this film [Figure 2(A)].

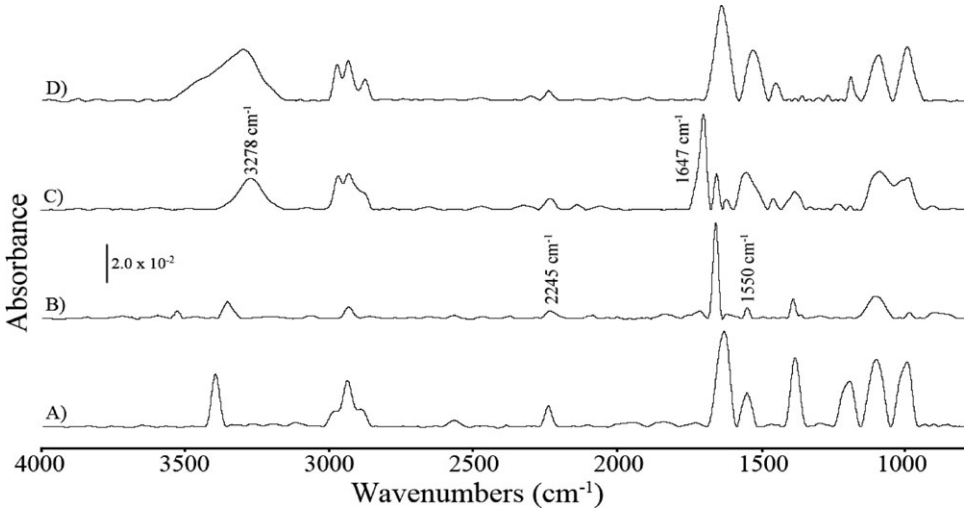

Figure 2. GA-FTIR spectra of bimolecular macroazoinitiator-immobilized silicon (A), oligoNIPAM (B), oligoNIPAM-COOH (C), and oligoNIPAM-OH (D).

Preparation of OligoNIPAM with —OH and —COOH End-Groups (Targeted Degree of Polymerization ≤10)

The surface-initiated NMP of NIPAM (1.0 g) was carried out in dry dichloromethane (30 mL) in a glass reactor, which was designed to hold three bimolecular macroazoinitiator-immobilized silicon wafers oriented normal to the base of the reactor. The chain transfer agent (changing amount of ME or MPA) was added to the reactor. To ensure smooth stirring and prevent damage to the surfaces of the substrates, we isolated the magnetic stirring bar at the center of device from the slides by a 1-cm-high glass O-ring. The solution was diluted to 30 mL volume with dry dichloromethane and degassed by purging with nitrogen for 20 min. The polymerization reaction was stirred vigorously at 50°C for 24 h. After polymerization, the substrates were removed from the solution and washed for several times with dichloromethane and then dried in a stream of nitrogen.

Instrumental Techniques

The grazing angle-Fourier transform infrared (GA-FTIR) spectra of the oligomeric brushes on silicon wafer were collected utilizing a Harrick Scientific GA-FTIR attachment coupled with a Thermo Nicolet 6700 spectrometer, collecting 128 sample scans, and utilizing Nicolet's OMNIC software. The X-ray photoelectron spectroscopy (XPS) measurements were done by a SPECS XPS spectrometer equipped with a Mg Kα X-ray source. After peak fitting of the C 1s spectra, all the spectra were calibrated in reference to the aliphatic C 1s component at a binding energy of 285.0 eV. The water contact-angle measurements were conducted at room temperature using a goniometer (DSA 100, Krüss) equipped with a microliter syringe. Deionized water (4 μL, 18 MΩ cm resistivity) was used as the wetting liquid. The morphology of the surfaces was recorded on an atomic force microscope (Park Systems XE70 SPM Controller LSF-100 HS). A triangular shaped Si_3N_4 cantilever with integrated tips (Olympus) was used to acquire the images in the noncontact mode. The normal spring constant of the cantilever was 0.02 N m^{-1}. The force between the tip and the sample was 0.87 nN. Gel permeation chromatography (GPC) analysis was performed with an Waters HPLC system consisting of a binary pump, an autosampler, a temperature controlled column oven and differential refractometer. The analytical separation was performed on Waters Styragel HR4 and HR6 columns (7.8 × 300 mm^2) at 27°C with a flow rate of 1 mL min^{-1}. THF was used as the mobile phase and the system was calibrated with narrow-disperse polystyrene standards (Shodex).

The ellipsometric measurements were conducted in ambient conditions using an ellipsometry (model DRE, EL X20C) equipped with a He-Ne laser (λ = 632.8 nm) at a constant incident angle of 75°. The average dry thickness of oligoNIPAM films with defined end-groups on silicon wafer was determined by fitting the data with a three-layer model (native silicon (refractive index, n = 3.86) + silicon oxide layer (n = 1.46) + oligoNIPAM (n = 1.47)).[38]

RESULTS AND DISCUSSION

Immobilization of Bimolecular Macroazoinitiator on Silicon Wafer

Ability of three methoxy silane functionalized organic molecules to form dense and ordered monolayers on a silicon substrate was extensively described in the literature.[28,39–41] In this study, the covalent attachment of bimolecular macroazoinitiator with three methoxy silane functional groups onto silicon surface was achieved by a self-assembly process. The bimolecular macroazoinitiator immobilization was confirmed with GA-FTIR [Figure 2(A)], XPS [Figure 3(A), Table I], ellipsometry, AFM [Figure 4(A)], and water contact-angle [Figure 4(A)] measurements. The presence of bimolecular macroazoinitiator on silicon surface was confirmed by the presence of bands at 1630, 2246, and 3393 cm^{-1}, which are assigned to C—O stretching, C≡N stretching, and N—H stretching vibrations, respectively [Figure 2(A)]. XPS analysis of the bimolecular macroazoinitiator monolayer [Figure 3(A), Table I] verifies the presence of O 1s, N 1s, and C 1s peaks curve fitted into the components with binding energies at about 533.8 eV (C—O) and 532.2 eV (C=O) for O 1s, 400.9 eV (N—H), and 400.2 eV (N=N) for N 1s, and 288.5 eV (C=O), 285.5 eV (C—N), 285.2 eV (C—O), and 285.0 eV (C—C/C—H) for C 1s. The thickness of bimolecular

Applied Polymer SCIENCE

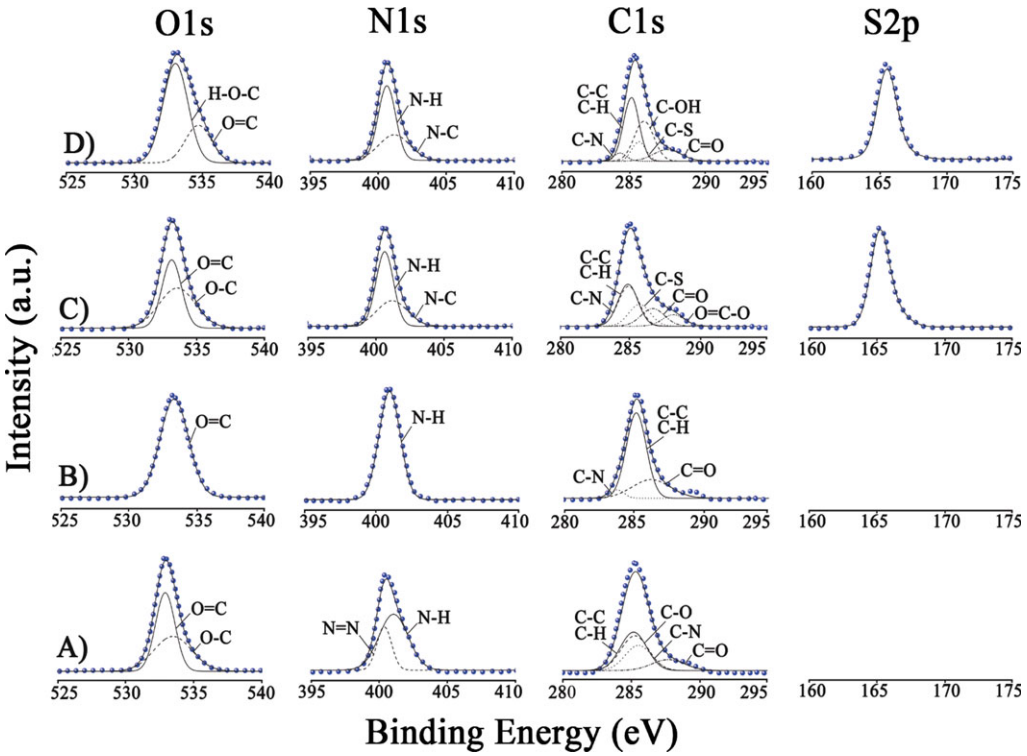

Figure 3. O 1s, N 1s C 1s, and S 2p core level XPS spectra recorded for bimolecular macroazoinitiator-immobilized silicon (A), oligoNIPAM (B), oligoNIPAM-COOH (C), and oligoNIPAM-OH (D). [Color figure can be viewed in the online issue, which is available at wileyonlinelibrary.com.]

macroazoinitiator layer was measured by ellipsometry at 2.8 ± 0.5 nm, this value is consistent with theoretical value (∼ 1.5 nm) obtained by *ab initio* calculations. Surface morphology of silicon substrate after the immobilization of bimolecular macroazoinitiator is shown in Figure 4(A). Analysis of bimolecular macroazoinitiator monolayer indicated a root-mean-square (rms) roughness of 0.35 nm. Finally, as illustrated by inset images in Figure 4(A), the immobilization of bimolecular macroazoinitiator induced a drastic change in surface wettability characterized by a large decrease of static water contact-angle from 5.0 ± 0.3° (hydroxylated silicon) to 80.8° ± 0.2° (bimolecular macroazoinitiator monolayer).

Table I. Atomic Concentrations and Binding Energies Given High-Resolution XPS for Initiator Immobilized Silicon Wafer and End-Functionalized OligoNIPAM Brushes Synthesized in CTA Solutions

	O1s		N1s			C1s					
Samples	C—O	C=O	N—H	N=N	N—C	C=O	C—O	C—S	C—N	C—C	S2p
Initiator layer											
Conc. (%)		23.9		14.7				61.4			
Energy (eV)	533.8	532.2	400.9	400.2		288.5	285.2		285.5	285.0	
oligoNIPAM											
Conc. (%)		18.7		9.1				72.2			
		533.7	400.7			286.1			284.0	285.0	
Energy (eV)											
oligoNIPAM-OH											
Conc. (%)		29.3		5.2				57.6			7.9
Energy (eV)	532.8	534.8	400.8		400.9	287.6	286.1	286.0	284.0	285.0	165.5
oligoNIPAM-COOH											
Conc. (%)		30.5		4.8				58.1			6.6
Energy (eV)	534.0	533.5	400.8		401.3	286.9	288.5	286.0	285.2	285.0	165.5

Binding energies are calibrated to aliphatic carbon at 285 eV.

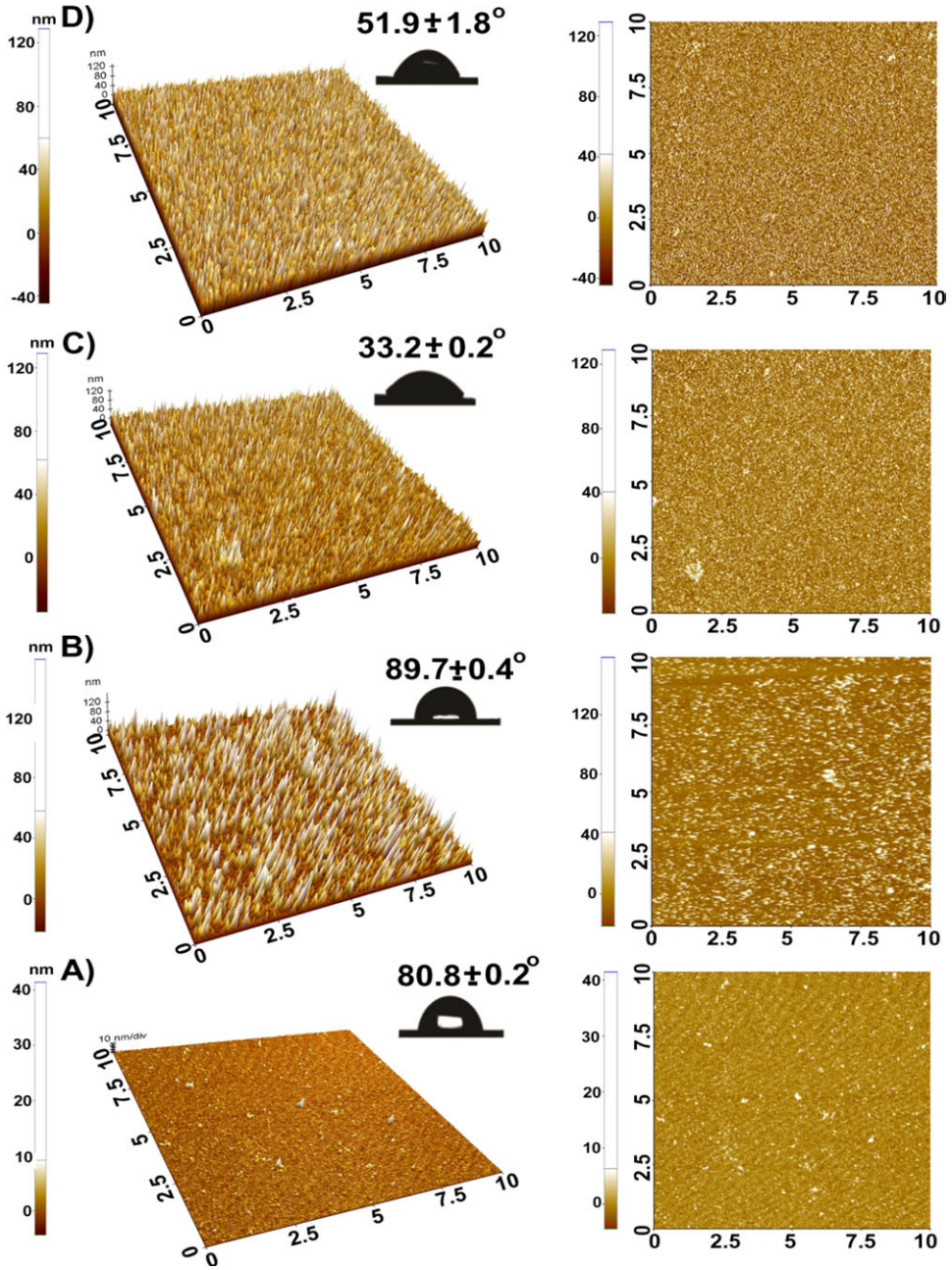

Figure 4. The 3D (left) and 2D (right) AFM topography images (10 × 10 μm^2, *z* scale is 10 nm) in ambient conditions and photographs of 4 μL water droplets (top) on the bimolecular macroazoinitiator-immobilized silicon (A), oligoNIPAM (B), oligoNIPAM-COOH (C), and oligoNIPAM-OH (D). [Color figure can be viewed in the online issue, which is available at wileyonlinelibrary.com.]

Formation of OligoNIPAM Brushes with —OH and —COOH End-Groups on Silicon Wafer via Surface-Initiated NMP

As mentioned in the Introduction, the surface-initiated NMP of NIPAM in the presence of chain transfer agent was carried out with the bimolecular macroazoinitiator modified silicon wafer. This method provided higher grafting densities compared with coupling reactions performed via "grafting to" method in solution, as excluded volume interactions, which restrict surface accessibility for oligomer chains, are screened out in the surface-initiated NMP. The oligomeric brushes are referenced according to functionalized end-groups, i.e., oligoNIPAM—OH and oligoNIPAM—COOH, where the —OH is for oligoNIPAM with hydroxyl end-group and —COOH for oligoNIPAM with carboxylic acid end-group. An illustration of immobilization of bimolecular macroazoinitiator onto silicon substrate and subsequent surface-initiated NMP to form oligoNIPAM—OH and oligoNIPAM—COOH brushes is shown in Scheme 1.

It has been reported that the addition of chain transfer agent into the reaction mixture provides a reliable route for the synthesis of polymer with a low molecular weight and a low polydispersity index (PDI).[42] Meanwhile, the fragmentation of

Applied Polymer SCIENCE

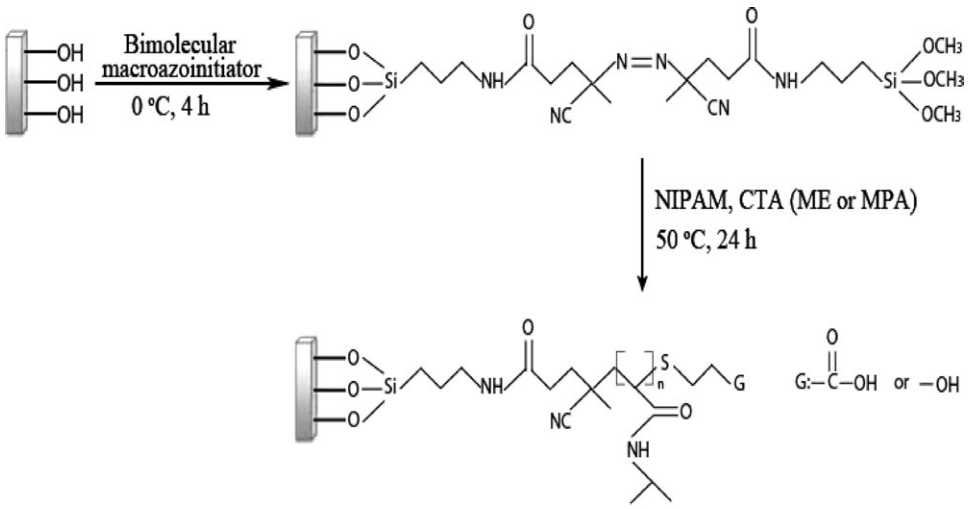

Scheme 1. Surface-initiated NMP of NIPAM in the presence of chain transfer agent.

immobilized bimolecular macroazoinitiator also allows for the formation of free oligomer in solution, the properties of which have been shown to correlate with the oligomer attached to the surface. As insufficient amount of oligomer degrafted from silicon surfaces for characterization, free oligomer can be analyzed to provide an approximation of the molecular weight properties of the immobilized chains. Because of possible entanglement of the free oligomer with immobilized chains, all samples were extracted in dichloromethane for 24 h to remove any untethered oligomer chains from the surface. Therefore, it is assumed that the molecular weights of the free and grafted oligomer chains are similar in our study. The oligomer formed in solution was isolated and characterized using GPC. In each case the GPC traces of the free oligomers (Figure 5) were monomodal and had narrow PDI values, which are characteristics of well-defined oligomers via surface-initiated NMP. For all oligomers synthesized, the PDIs are all below 1.19, indicating that in each case the polymerization was controlled. Moreover, the molecular weight of the oligomer in solution appears to relate well to thickness of the oligomer attached to the silicon wafer. For example, in the case of the oligoNIPAM-OH or oligoNIPAM-COOH brushes, the number-average molar weight ($\overline{M}_n$) of the oligomers in solution were 800 and 1000 g mol^{-1}, which corresponded to oligomer brush thicknesses of 7.1 ± 0.4 and 8.9 ± 0.3 nm, respectively. In case of the oligoNIPAM, the $\overline{M}_n$ was 1600 g mol^{-1}, which correspond to an oligomer brush thickness of 15.1 ± 0.2 nm.

The brush thickness (h, nm) is proportional to the $\overline{M}_n$ of the free oligomer simultaneously produced in the solution ($h = \sigma\overline{M}_n/\rho N_A 10^{-21}$ where σ(chains nm^{-2}) is the grafting density, ρ (1.35 g cm^{-3}) is the density of oligomer and N_A (6.02 × 10^{23} mol^{-1}) is Avogadro's number),[43] suggesting uniform growth of graft chains with a constant density. From the thickness-versus-$\overline{M}_n$ curve, grafting density, σ (chains nm^{-2}), was estimated to be about 8.14 chains nm^{-2}. In this estimation, average distance between grafting points, D (nm) ($D = (4/\pi\sigma)^{1/2}$),[43] was found to be 0.39 nm. The radius of gyration (R_g, nm) of the oligoNIPAM was estimated using the equation: $R_g = b(\overline{DP}_n/6)^{1/2}$ where $\overline{DP}_n$ is the degree of polymerization and b, is the segment length (assumed to be 0.3 nm for oligoNIPAM).[44] An indication of having oligomeric brush surfaces can be when the interchain distance is less then the radius of gyration of the corresponding free oligomer chain.[45] The radius of gyration of oligoNIPAM, oligoNIPAM-OH, and oligoNIPAM—COOH was calculated as 0.46, 0.32, and 0.36 nm, respectively. We have achieved high grafting densities for all samples, and the overall interchain grafting distance in all cases is less than the radius of gyration of these free oligoNIPAM chains in solution, indicating that the chains are indeed in a stretched brush-like conformation.

OligoNIPAM film morphology was studied by conducting AFM measurements in ambient conditions [Figure 4(B–D)]. The comparison with Figure 4(A) evidenced significant topography change and surface roughness resulting from polymer formation. Indeed, oligoNIPAM brushes appear as needle-like structures homogeneously distributed over the entire substrate area. Similar morphologies were observed for the oligoNIPAM—OH and oligoNIPAM—COOH brushes, however, with random distributions of apparent needle-like structures. The rms roughness of oligoNIPAM brushes was 1.46 nm, whereas those of oligoNIPAM—OH and oligoNIPAM—COOH brushes were 0.78 and 1.01 nm, respectively, indicated the decrease of surface roughness in the presence of chain transfer agent. These results

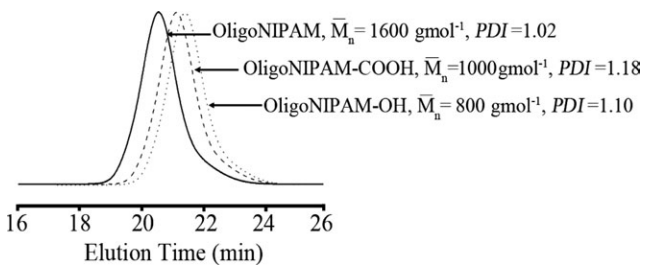

Figure 5. Evolution of GPC traces of oligoNIPAM, oligoNIPAM-COOH, and oligoNIPAM-OH synthesized in solution.

suggest that the functional oligoNIPAM coatings grown by surface-initiated NMP in the presence of chain transfer agent from bimolecular immobilized silicon surface are dense and highly homogeneous brushes, as opposed to the coil or mushroom configurations[46] that are likely obtained upon grafting functionalized polymers from solution.

The oligoNIPAM chains with functional end-group also lead to characteristic changes in the polarity of the surfaces that are directly reflected in wetting behavior. Therefore, we performed water contact-angle measurements to quantify the corresponding changes for each oligomer brushes with different end-group. The static water contact-angle of oligoNIPAM was found to be 89.7° ± 0.4° [Figure 4(B)]. The incorporation of —OH and —COOH functional groups into the oligoNIPAM chains as end-group caused to the increase of surface hydrophilicity. In this case, the static water contact-angle of oligoNIPAM—OH and oligoNIPAM—COOH decreased substantially to about 51.9° ± 1.8° and 33.2° ± 0.2°, respectively, consistent with the hydrophilic nature of these surfaces [Figure 4(C,D)].

To further characterize oligoNIPAM brushes, samples were then analyzed using GA-FTIR and XPS. GA-FTIR spectra of oligoNIPAM—OH and oligoNIPAM—COOH brushes are represented in Figure 2(C,D). In all cases, we clearly observed the amide I band (1647 cm^{-1}, (C=O stretching) and amide II band (1550 cm^{-1}, N—H stretching). The presence of two bands at 1367 and 1388 cm^{-1} are associated with the deformation of two methyl groups on isopropyl [Figure 2(B)].[44] A carboxylic acid band at 3278 cm^{-1} in the GA-FTIR spectrum [Figure 2(C)] reflects the formation of a oligoNIPAM—COOH, whereas a broad hydroxyl band at 3500–3300 cm^{-1} [Figure 2(D)] indicates the formation of a oligoNIPAM—OH.

Elementary composition and values of binding energies given by XPS are summarized in Table I. Detailed O 1s, N 1s, C 1s, and S 2p core level spectra recorded for oligoNIPAM brushes with different end-groups are also displayed in Figure 3(B–D). They show the typical fingerprint of oligoNIPAM backbone[47] with binding energies recorded at 533.7 eV (C=O) for O 1s, 400.7 eV (N—H) for N 1s, and 286.1 eV (C=O), 284.0 eV (C—N) and 285.0 eV (C—C/C—H) for C 1s. More specific signal was the small S 2p peak at about 165 eV (C—S), indicating the formation of oligoNIPAM brushes with —OH and —COOH end-groups.

CONCLUSIONS

In conclusion, for the first time to our knowledge, surface-initiated NMP in the presence of chain transfer agent has been utilized by the bimolecular macroazoinitiator-anchored silicon wafer to prepare oligoNIPAM brushes with different end-groups. The fragmentation of immobilized bimolecular macroazoinitiator resulted in the formation of free oligomer in solution, which was characterized and confirmed the formation of well-defined oligomers. In each cases, film thicknesses correlated well with experimental molecular weights of free oligomer chains. The possibility to tune the surface properties (e.g., film thickness, grafting density, wettability, and surface morphology) by using different chain transfer agents was also demonstrated. Unlike other grafting process, surface-initiated NMP technique in the presence of chain transfer agent can be advantageously applied to the production of oligomer brushes with different end-groups. Studies of the stimuli responsive behavior of oligoNIPAM brushes are currently under investigation in our laboratory and will be the subject of an upcoming report.

REFERENCES

1. Wadhwa, G. *J. Sci. Ind. Res.* **1990**, *49*, 486.
2. Hoffman, A. S. *Clin. Chem.* **2000**, *46*, 1478.
3. Lasseter, T. L. *Analyst* **2004**, *129*, 3.
4. Williams, R. A.; Blanch, H. W. *Biosens. Bioelectron.* **1994**, *9*, 159.
5. Caster, D. G.; Ratner, B. D. *Surf. Sci.* **2002**, *500*, 28.
6. Jenney, C. R.; Anderson, J. M. *J. Biomed. Mater. Res.* **1999**, *46*, 11.
7. Lind, M.; Overgaard, S.; Soballe, K.; Nguyes, T.; Ongpipattankul, B.; Bunger, C. J. *Orthop. Res.* **1996**, *14*, 343.
8. Mann, B. K.; Tsai, A. T.; Scott-Burden, T.; West, J. L. *Biomaterials* **1999**, *20*, 2281.
9. Zhao, B.; Brittain, W. J. *Prog. Polym. Sci.* **2002**, *99*, 677.
10. Zheng, G.; Stover, H. D. H. *Chin J. Polym. Sci.* **2003**, *21*, 639.
11. Edmondson, S.; Osborne, V. L.; Huck, W. T. S. *Chem. Soc. Rev.* **2004**, *33*, 14.
12. Guerrini, M. M.; Charleux, B.; Vairon, J. P. *Macromol. Rapid Commun.* **2000**, *21*, 669.
13. Ayres, N.; Haddleton, D. M.; Shooter, A. J.; Pears, D. A. *Macromolecules* **2002**, *35*, 3849.
14. Bontempo, D.; Tirelli, N.; Feldman, K.; Masci, G.; Crescenzi, V.; Hubbell, J. A. *Adv. Mater.* **2002**, *14*, 1239.
15. Kizhakkedthu, J. N.; Brooks, D. E. *Macromolecules* **2003**, *36*, 591.
16. Zheng, G.; Stover, H. D. H. *Macromolecules* **2003**, *36*, 1808.
17. Turan, E.; Demirci, S.; Caykara, T. *Thin Solid Films* **2010**, *518*, 5950.
18. Turan, E.; Caykara, T. *J. Polym. Sci. Part A: Polym. Chem.* **2010**, *48*, 3880.
19. Ozturk, E.; Turan, E.; Caykara, T. *Appl. Surf. Sci.* **2010**, *257*, 1015.
20. Barner, L.; Li, C.; Hao, X.; Stenzel, M. H.; Barnel-Kowollok, C.; Davis, T. P. *J. Polym. Sci. Part A: Polym. Chem.* **2004**, *42*, 5067.
21. Perrier, S.; Takolpuckdee, P.; Mars, C. A. *Macromolecules* **2005**, *38*, 6770.
22. Gurbuz, N.; Demirci, S.; Yavuz, S.; Caykara, T. *J. Polym. Sci. Part A: Polym. Chem.* **2011**, *49*, 423.
23. Hodges, J. C.; Harikrishnan, L. S.; Ault-Justus, S. *J. Comb. Chem.* **2000**, *2*, 80.
24. Bian, K.; Cunningham, M. F. *J. Polym. Sci. Part A: Polym. Chem.* **2005**, *43*, 2145.
25. Husseman, M.; Malmstrom, E. E.; McNamara, M.; Mate, M.; Mecerreyes, D.; Benoit, D. G. *Macromolecules* **1999**, *32*, 1424.

26. Chaumont, P.; Chapel, J. P.; Devaux, C.; Beyou, E. *Polym. Prepr.* **2002**, *43*, 74.
27. Kasseh, A.; Ait-Kadi, A.; Reiedl, B.; Pierson, J. F. *Polymer* **2003**, *44*, 1367.
28. Bartholome, C.; Beyou, E.; Bourgeat-Lami, E.; Chaumont, P.; Zydowicz, N. *Polymer* **2005**, *46*, 8502.
29. Bian, K.; Cunningham, M. F. *Polymer* **2006**, *47*, 5744.
30. Heskins, M.; Guillet, J. E. *J. Macromol. Sci. A.* **1968**, *2*, 1441.
31. Bae, Y. H.; Okano, T.; Kim, S. W. *J. Polym. Sci. Part B: Polym. Phys.* **1990**, *28*, 923.
32. Zhang, J.; Pelton, R. *Colloids Surf.* **1999**, *156*, 111.
33. Yim, H.; Kent, M. S.; Huber, D. L. *Macromolecules* **2003**, *36*, 5244.
34. Cheng, X.; Canavan, H. E.; Graham, D. J.; Castner, D. G.; Ratner, B. D. *Biointerphase* **2006**, *1*, 61.
35. Huber, D. L.; Manginell, R. P.; Samara, M. A. B.; Kim, I.; Bunker, B. C. *Science* **2003**, *301*, 352.
36. Hu, J.; Wang, M.; Weier, H. U. G.; Frantz, P.; Kolbe, W.; Ogletree, D. F.; Salmeron, M. *Langmuir* **1996**, *12*, 1697.
37. Smith, A. D. *Macromol. Chem.* **1967**, *103*, 301.
38. Plunkett, K. N.; Zhu, X.; Moore, J. S.; Leckband, D. E. *Langmuir* **2006**, *22*, 4259.
39. Ghannam, L.; Parvole, J.; Laruelle, G.; Francois, J.; Billon, L. *Polym. Int.* **2006**, *55*, 1199.
40. Topham, P. D.; Howse, J. R.; Crook, C. J.; Parnell, A. J.; Geoghegan, M.; Jones, R. A.; Ryan A. J. *Polym. Int.* **2006**, *55*, 808.
41. Demirci, S.; Caykara, T. *Surf. Sci.* **2010**, *604*, 649.
42. Turan, E.; Caykara, T. *J. Polym. Sci. Part A: Polym. Chem.* **2011**, *49*, 2818.
43. Luzinov, I.; Julthongpiput, D.; Malz, H.; Pionteck, J.; Tsukruk, V. V. *Macromolecules* **2000**, *33*, 1043.
44. Zhu, X.; Yan, C.; Winnik, F. M.; Leckband, D. *Langmuir* **2007**, *23*, 162.
45. de Gennes, P. G. *Macromolecules* **1980**, *13*, 1069.
46. Montagne, F.; Polesel-Maris, J.; Pugin, R.; Heinzelmann, H. *Langmuir* **2009**, *25*, 983.
47. Xu, F. J.; Zhong, S. P.; Yung, L. Y. L.; Kang, E. T.; Neoh, K. G. *Biomacromolecules* **2004**, *5*, 2392.